

# RSC Advances

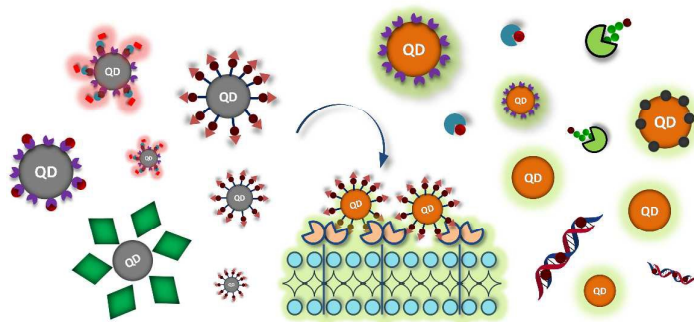


This is an *Accepted Manuscript*, which has been through the Royal Society of Chemistry peer review process and has been accepted for publication.

*Accepted Manuscripts* are published online shortly after acceptance, before technical editing, formatting and proof reading. Using this free service, authors can make their results available to the community, in citable form, before we publish the edited article. This *Accepted Manuscript* will be replaced by the edited, formatted and paginated article as soon as this is available.

You can find more information about *Accepted Manuscripts* in the [Information for Authors](#).

Please note that technical editing may introduce minor changes to the text and/or graphics, which may alter content. The journal's standard [Terms & Conditions](#) and the [Ethical guidelines](#) still apply. In no event shall the Royal Society of Chemistry be held responsible for any errors or omissions in this *Accepted Manuscript* or any consequences arising from the use of any information it contains.



Recent progress in quantum dot (QD) based chemo- and biosensors for various applications is summarized.

## Recent progress in quantum dot based sensors

Cite this: DOI: 10.1039/x0xx00000x

Lei Cui,<sup>a</sup> Xiao-Peng He<sup>\*b</sup> and Guo-Rong Chen<sup>\*b</sup>

This review summarizes the recent progress in quantum dot (QD) based sensors used for the photoluminescent detection of a variety of species *in vitro* and *in vivo*. New trends in using these nanomaterials for sensing applications are highlighted.

Received 00th January 2015,  
Accepted 00th January 2015

DOI: 10.1039/x0xx00000x

www.rsc.org/

### 1. Introduction

Quantum dots (QDs) are defined as semiconductor nanomaterials that emit photoluminescence (PL) with a tuneable wavelength.<sup>1</sup> QDs have been traditionally used in the production of solar cells, transistors, LEDs, etc. However, they have also shown a good promise for use in the fabrication of sensors. Owing to their unique and easily tunable optical properties, QD based chemo- and bio-sensors have been vividly developed since the 21<sup>st</sup> century.<sup>2</sup>

Traditional materials for sensor development include fluorescence organic dyes,<sup>3,4</sup> transition metal complexes<sup>5,6</sup> and carbon materials such as carbon nanotube<sup>7-9</sup> and graphene.<sup>10</sup> Recently, there also generates a new trend in using few-layer transition metal chalcogenides as the substrate to fabricate optical sensors.<sup>11</sup> Comparison with these materials, QD is believed to be superior in terms of its luminescence lifetimes, resistances against photobleaching, narrow emission bands, and especially its broad absorption bands that allow for a diverse selection of possible excitation wavelengths from the visible to the near infrared regions.<sup>12</sup> These features make QDs an ideal choice for the versatile design of sensors.

The following content will summarize the functionalization and application of QDs in the optical sensing of a variety of species, both *in vitro* and *in vivo*. We note that this review mainly covers QD based sensors developed during the past two years (2013 and 2014). New trends in using these materials as sensors are highlighted.

### 2. QD based chemosensors

#### 2.1. QD based chemosensors for ions

Transition metal ions are important natural elements, which play important roles in a multitude of biological processes. However, the excess of these ions is harmful. As a consequence, QD based PL sensors for transition metal ion detection have been actively developed.

The main principle for sensor construction relies on the functionalization of QDs with a selective ion receptor. On the one hand, after the specific receptor-ion interaction, the PL of the QDs could be quenched probably due to selective collisions between the ion and receptor, leading to QD aggregation as a result of the loss of receptor on the surface. Charge transfer between transition metal and the capping agent on the surface might also cause a PL quenching.<sup>13</sup> On the other hand, ratiometric and PL “off-on” sensors were developed based on QDs, the rationale of which are described in detail within the context below.

Glutathione (GSH)<sup>13,14</sup> and mercaptoacetic acid (MAA)<sup>15</sup> were used as receptors for copper ions (Cu<sup>2+</sup>) to coat CdTe or ZnSe QDs. The PL of the coated QDs could be quenched selectively in the presence of Cu<sup>2+</sup> (Fig. 1). To understand the kinetics of the PL quenching of cysteine-coated CdS QDs with Cu<sup>2+</sup>, model free chemometrics methods were employed.<sup>16</sup> This study provided a useful insight into the simultaneous determination of multiple analytes.

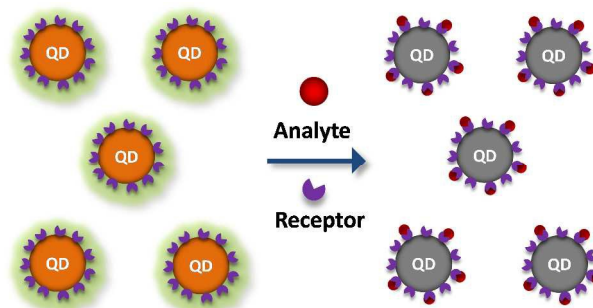


Figure 1. Detection of analyte using receptor coated QDs.

QDs without capping a receptor were also used for Cu<sup>2+</sup> detection (Fig. 2). Several cations, such as Cu<sup>2+</sup>, Ag<sup>+</sup> and Hg<sup>2+</sup>, have been determined to possess the ability to replace the

$\text{Cd}^{2+}$  ions on the surface of CdSe QDs. However, use of thiosulfate was shown to eliminate the interference of  $\text{Ag}^+$  and  $\text{Hg}^{2+}$  for  $\text{Cu}^{2+}$  probably by forming a passivation layer on the QD surface, resisting the competing ions.<sup>17</sup> Comparison with heavy-metal based QDs, other QDs that might be less toxic were prepared. A ZnO QD whose PL can be quenched selectively by  $\text{Cu}^{2+}$  was incorporated into a portable miniature probe, which showed sub micromolar limit of detection (LOD) and a high upper detection concentration.<sup>18</sup> A label-free Si-QD was synthesized, which showed PL quenching with the hydroxyl radicals produced by a Fenton reaction involving  $\text{Cu}^{2+}$ , ascorbic acid and  $\text{H}_2\text{O}_2$ .<sup>19</sup>

Particle size was observed to control the quenching efficiency of cysteine coated CdTe QDs with  $\text{Ag}^+$ .<sup>20,21</sup> A larger size facilitated the sensitivity and selectivity probably because of the lower passivation of surface traps by  $\text{Ag}^+$  adsorption. This size-effect was claimed to be equally important for other QD based optical sensors. Mercaptosuccinic acid coated CdS QDs showed a quenched PL in the presence of different metal ions, and were used to determine  $\text{Hg}^{2+}$  in an artificial aqueous sample.<sup>22</sup>

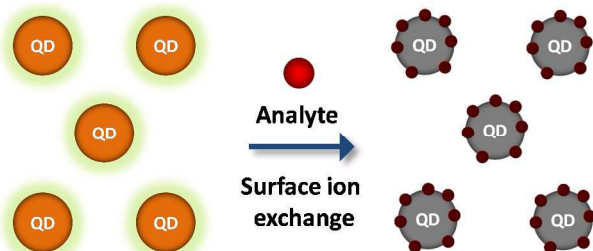


Figure 2. Detection of analyte using receptor-free QDs.

Besides the fluorimetric detection rationale, a ratiometric CdTe/CdS QD based sensor was developed for  $\text{Hg}^{2+}$ .<sup>23</sup> A red-emitting QD was embedded in silica nanoparticles on which a green-emitting QD coated by GSH was covalently coupled. The green emission could be selectively quenched by  $\text{Hg}^{2+}$  with the red emission retained (Fig. 3), which enabled the detection of mercury ions in biological fluids in a ratiometric way.

PL-quenching based, organic acid-coated QDs were developed for  $\text{Co}^{2+}$ ,<sup>24,25</sup>  $\text{Fe}^{2+}$ ,<sup>26</sup> and  $\text{Cr}^{3+}$ .<sup>27,28</sup> CdSe QDs decorated on the tip of an optical fiber in a sol-gel matrix were also used for the selective detection of  $\text{Cr}^{3+}$ .<sup>29</sup> Considering the importance of  $\text{Zn}^{2+}$  implicated in many pathological processes, QDs functionalized with  $\text{Zn}^{2+}$  receptors have been constructed. Carboxymethyl chitosan was used to coat CdTe QDs by electrostatic interactions.<sup>30</sup> Following the strong binding between surface-confined chitosan and  $\text{Zn}^{2+}$ , the ion could prevent nonradiative relaxations of the QDs, leading to enhancement of the PL. The positively charged chitosan could also facilitate the endocytosis of the QDs for the imaging of  $\text{Zn}^{2+}$  in prostate cancer cells. 8-aminoquinoline, a known  $\text{Zn}^{2+}$  receptor, was used to covalently coat the surface of QDs. The interaction of the molecule with a  $\text{CuInS}_2$  dot led to suppression of its PL probably by disruption of the radiative recombination process.<sup>31</sup> Then, chelation with  $\text{Zn}^{2+}$  using the lone pair electrons of the N atom of 8-aminoquinoline inhibited the quenching process, leading to recovery of the PL. A  $\text{SiO}_2$ -S-Zn-CdS QD with a suppressed PL

induced by  $\text{S}^{2-}$  was prepared, and the presence of  $\text{Zn}^{2+}$  or  $\text{Cd}^{2+}$  enhanced the PL by formation of ZnS or CdS passivation layer around the QDs.<sup>32</sup>

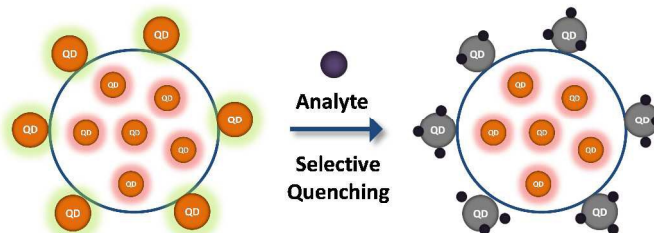


Figure 3. Detection of analyte using ratiometric QDs sensor.

$\text{Pb}^{2+}$  is among the most toxic heavy metals. However, because of the self-luminescence of serum proteins excited by visible light, sensors that can detect the ion in serum samples have been rare. A near infrared (NIR, which eliminates protein auto-luminescence), fluorescence resonance energy transfer (FRET) based sensor for  $\text{Pb}^{2+}$  was developed using an up-conversion  $\text{NaYF}_4:\text{Yb}^{3+}/\text{Tm}^{3+}$  nanoparticle as the energy donor and CdTe QDs as the energy acceptor.<sup>33</sup> The sensor showed good linear Stern-Volmer characteristics and nanomolar LOD for  $\text{Pb}^{2+}$  in a serum sample. In contrast, silica coated ZnS QD for  $\text{Pb}^{2+}$  based on PL quenching was reported.<sup>34</sup>

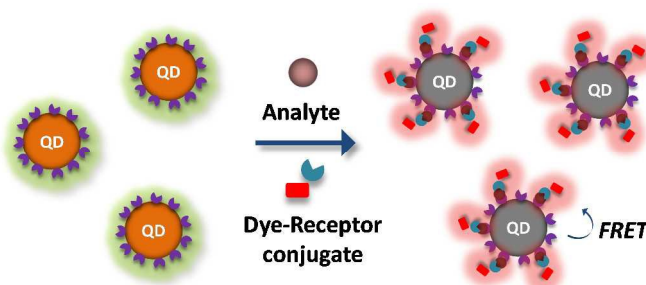


Figure 4. Detection of analyte based on FRET between QDs and dyes.

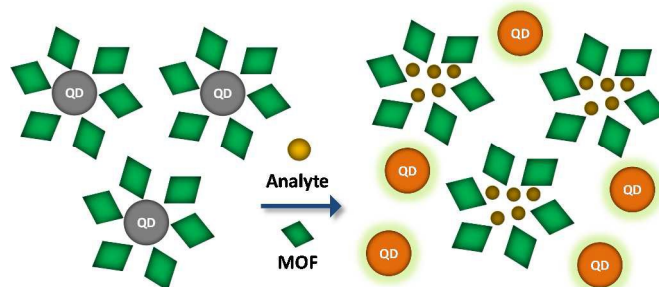


Figure 5. Detection of analyte using MOF-QDs construct.

A 15-crown-5-ether coated CdSe/ZnS QD was constructed for ratiometric detection of  $\text{K}^+$ .<sup>35</sup> Through conjugation with a crown-coupled rhodamine B selectively mediated by  $\text{K}^+$ , the PL

of QDs decreased and the fluorescence of rhodamine increased due to the FRET mechanism (Fig. 4). Metal-organic frameworks (MOFs) have attracted intensive interest in many research areas. A MOF construct was used to cage a ZnO QD by electrostatic interactions, quenching its PL by electron transfer (ET) processes.<sup>36</sup> Subsequently, only the addition of sodium phosphate, among other species, collapsed the MOF-QD complex, which led to recovered PL of QDs (Fig. 5). The properties of the QD based ion sensors reviewed in this section are listed in Table 1.

**Table 1.** Properties of the QD based sensors for ions.

Analyte	Structure	CA <sup>a,b</sup>	LOD (μM) <sup>c</sup>	Ref <sup>e</sup>
	CdTe	GSH	0.67 <sup>d</sup>	13
	ZnSe	GSH	0.0001	14
	ZnSe	MAA	0.47	15
Cu <sup>2+</sup>	CdS	L-Cysteine	0.013	16
	CdSe/ZnS	CTAB	0.00014	17
	ZnO	n.a.	0.768	18
	Silicon	n.a.	0.008	19
	CdTe	Homocysteine	0.008	20
Ag <sup>+</sup>	CdTe	MSA	0.054	21
	CdS	MSA	0.51	22
Hg <sup>2+</sup>	CdTe/CdS	MPA	0.31	23
	Mn-doped ZnS	NAC	0.06	24
Co <sup>2+</sup>	CuInS <sub>2</sub> /ZnS	TGA	0.16	25
	CdTe	TGA	0.12	26
Fe <sup>2+</sup>	CdTe	MPA/TGA	n.a.	27
	Mn-doped ZnS	Protein	0.003	28
	CdSe	MPTMS	0.03	29
Zn <sup>2+</sup>	CdTe	Chitosan	4.5	30
	CuInS <sub>2</sub>	MPA	4.5	31
	SiO <sub>2</sub> -S-Zn-CdS	GSH	2.0	32
Pb <sup>2+</sup>	NaYF <sub>4</sub> :Yb <sup>3+</sup> /Tm <sup>3+</sup> /CdTe	TGA	0.008	33
	ZnS	Silica	n.a.	34
K <sup>+</sup>	CdSe/ZnS	15C5E	4.3	35
Phosphate	ZnO	APTMS	0.053	36

<sup>a</sup>CA means capping agent; <sup>b</sup>Abbreviation: GSH = glutathione; MAA = mercaptoacetic acid; CTAB = hexadecyl trimethylammonium bromide; n.a. = not available; MSA = mercaptosuccinic acid; MPA = 3-mercaptopropionic acid; NAC = N-acetyl-L-cysteine; TGA = thioglycolic acid; MPTMS = 3-mercaptopropyltrimethoxysilane; 15C5E = 15-crown-5-ether; APTMS = (3-aminopropyl) trimethoxysilane; <sup>c</sup>LOD means limit of detection; <sup>d</sup>μg mL<sup>-1</sup>; <sup>e</sup>Reference (Ref) number cited in the main text.

## 2.2. QD based chemosensors for small molecules

Detection of biologically important small molecules such as amino acids and natural products may aid not only basic research, but also disease diagnosis. The rationale for the sensing generally depends on the decoration of QDs with a receptor (Fig. 6) or with a molecularly imprinted polymer (MIP, a method to make artificial receptors, Fig. 7) for the small molecule of interest. After the specific receptor-ligand recognition, the PL of the QD can be tuned (either turn-on or turn-off) as elaborated in the following context.

Amino acids and small peptides are important regulators of physiological processes. On the basis of competitive ligand-receptor binding, "turn-on" QD sensors were developed for histidine (Fig. 6). Nickel<sup>37</sup> and manganese<sup>38</sup> were used to coor-

inate with dopamine-coated and GSH-coated QDs quenching the PL, respectively. Both systems showed a recovered PL in the presence of histidine because of the competitive binding of the metal ions with the amino acid.

An MIP (Fig. 7) was covalently linked to a QD, which showed better cysteine recovery rates from serum samples than unmodified QDs.<sup>39</sup> GSH, a tripeptide, is over-expressed in some cancer cells. Sensitive detection of GSH will facilitate cancer diagnosis. Upconversion QDs were coated with quinones to quench the PL. Then, addition of GSH reduced the quinones, inhibiting the electron-transfer (from QDs to quinone) induced quenching of QDs.<sup>40,41</sup>

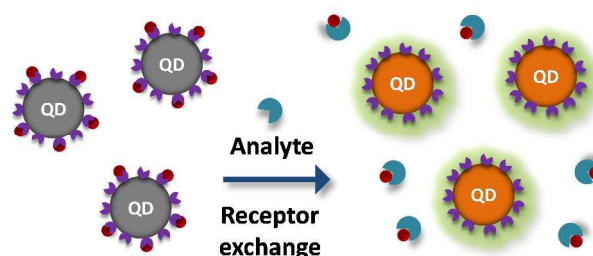


**Figure 6.** Detection of analyte based on competitive ligand-receptor binding.

Polyphenols are among the most abundant antioxidants in our diet. Considering that they possess a diverse range of biological activities, sensitive tracking of the amount of polyphenols in our body is important. The rationale on which to design QD based polyphenol sensors mainly relies on the electron-transfer induced quenching mechanism (Fig. 8). With this principle enzyme-coated,<sup>42</sup> MIP-capped,<sup>43,44</sup> and thioglycolic acid-capped<sup>45</sup> QDs were constructed for sensing catechin, trichlorophenol and kaempferol, respectively.

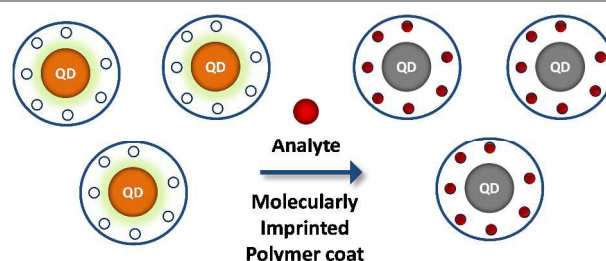


**Figure 7.** Detection of analyte based on QDs coated with molecularly imprinted polymers.

Free radicals are another class of important signalling species in the human body. On the basis of PL quenching, QD-hyperbranched polyether hybrid nanospheres<sup>46</sup> and ZnO QDs<sup>47</sup> were constructed for detection of nitroxide radicals. Boronate-coated CuInS<sub>2</sub> QDs<sup>48</sup> and wurtzite CuGaS<sub>2</sub> QDs<sup>49</sup> were prepared for dopamine and L-noradrenaline, respectively, based on PL quenching similarly. In contrast, a PL "turn-on" CdTe/CdS/ZnS QD sensor with surface-attached KMnO<sub>4</sub> was used to determine L-ascorbic acid in human urine samples.<sup>50</sup> FRET was also used to construct QD sensors for small molecules. A bovine serum albumin (BSA)-conjugated 17β-estradiol was used to

covalently coat a QD.<sup>51</sup> Then, by a competitive binding between free 17 $\beta$ -estradiol and the surface-confined 17 $\beta$ -estradiol with a fluorescent aptamer, the PL of the QDs could be quenched due to FRET. FRET was also shown to tune the PL of mercaptopropionic acid coated CdS QDs upon interaction with vitamin B<sub>12</sub>, facilitating pharmaceutical and biomedical analyses of the natural product.<sup>52</sup>

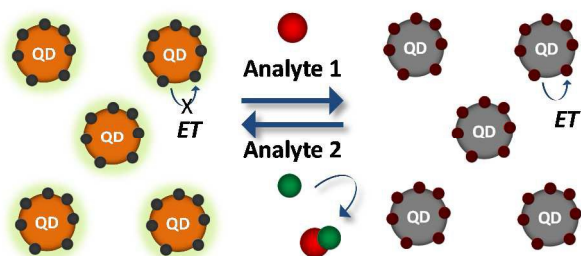


**Figure 8.** Detection of analyte based on the reversible electron transfer (ET) mechanism.

**Table 2.** Properties of the QD based sensors for small molecules.

Analyte	Structure	CA <sup>a,b</sup>	LOD ( $\mu\text{M}$ ) <sup>c</sup>	Ref <sup>e</sup>
L-Histidine	CdTe	MPA	0.5	37
Histidine	CdTe	GSH	0.00182 <sup>d</sup>	38
Cysteine	CdTe	MIP	0.85	39
GSH	NaYF <sub>4</sub> :Yb	PAA	0.29	40
	CdTe	MPA	0.0065	41
Polyphenol	CdTe	Enzyme	0.001 <sup>d</sup>	42
	Mn-doped ZnS	MIP	n.a.	43
	CdTe	MIP	0.00025 <sup>d</sup>	44
NO	CdTe	TGA	0.79 <sup>d</sup>	45
	CdSe	Polyether	0.025	46
	Radical	ZnO	n.a.	n.a.
Dopamine	CuInS <sub>2</sub>	MCA	0.2	48
L-Noradrenaline	CuGaS <sub>2</sub>	MCA	0.5	49
L-Ascorbic acid	CdTe/CdS/ZnS	NAC	0.0018	50
Estradiol	Qdot 605 ITK <sup>TM</sup>	n.a.	0.00022	51
Vitamin B <sub>12</sub>	CdS	MPA	6.91 <sup>d</sup>	52
	CdSe/ZnS	Antibody	0.0003 <sup>d</sup>	53
	CuInS <sub>2</sub>	MPA	0.06	54
	CdTe/CdS	TGA	0.08	55
Toxic chemicals	Mn-doped ZnS	MPA	0.0032 <sup>d</sup>	56
	CdTe	MIP	0.4	57
	Mn-doped ZnS	MIP	0.009	58
	CuInS <sub>2</sub>	MPA	0.6	59

<sup>a</sup>CA means capping agent; <sup>b</sup>Abbreviation: MPA = 3-mercaptopropionic acid; GSH = glutathione; MIP = molecular imprinted polymer; PAA = polyacrylic acid; TGA = thioglycolic acid; NAC = *N*-acetyl-L-cysteine; <sup>c</sup>LOD means limit of detection; <sup>d</sup> $\mu\text{g mL}^{-1}$ ; <sup>e</sup>Reference (Ref) number cited in the main text.

Meanwhile, QD based detections for toxic chemicals have been carried out. A solid-phase immunoassay was developed, using two antibody-coated QDs with different emission wavelengths, for the simultaneous quantification of clothianidin and thiacloprid in real samples.<sup>53</sup> CuS<sub>2</sub> QDs stabilized with mercaptopropionic acid was synthesized, which showed a quenched PL in the presence of Pb<sup>2+</sup>.<sup>54</sup> This QD sensor was used to detect parathion-methyl (PM). PM can be hydrolyzed by organophos-

phorus hydrolase, producing di-methylthiophosphoric acid to bind Pb<sup>2+</sup> ions on the QD surface, thus recovering the PL.

Gold nanoparticles (AuNPs) were used as an FRET acceptor for QDs to construct PL sensor for melamine (that has stronger bind affinity for AuNPs than for QDs) contamination in milk productions.<sup>55</sup> Melamine, while confined on QD surface, was used alternatively as a receptor for clenbuterol in biological fluids, producing a quenched PL due to aggregation.<sup>56</sup> MIP coated QDs were prepared to sense both melamine and clenbuterol through PL quenching,<sup>57</sup> and the mechanism was also exploited for sensing toxic chemicals such as cyphenothrin<sup>58</sup> and dicyandiamide.<sup>59</sup> The properties of the QD based small-molecule sensors reviewed in this section are listed in Table 2.

### 3. QD based biosensors

#### 3.1. QD based biosensors for biomolecules

Use of QDs for the detection of biomolecules such as DNA, protein and saccharide has been an active research area. Replacement assay represents the most employed tactic to construct the sensors. For example, QDs decorated with a ligand-quencher conjugate show a turn-on PL upon interaction of the conjugate with the test biomolecule (Fig. 10). Sophisticated QD sensors with a surface-immobilized redox center have also been developed to tune the PL of QDs by electron transfer (Fig. 11), enabling the photoluminescent probing of biomolecules on both the molecular and cellular levels.

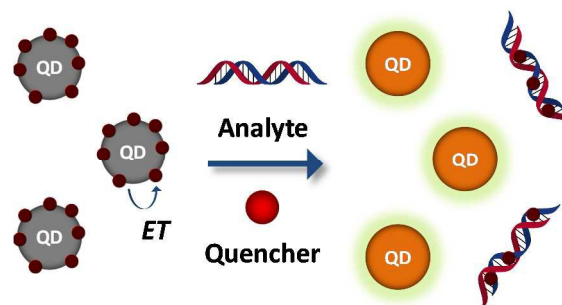


**Figure 9.** Detection of DNA using the QD PL “turn off-on” rationale.

Because of their high binding affinity and specificity for DNA, organometallic compounds were used for conjugation with QDs. Ruthenium<sup>60</sup> and platinum<sup>61</sup> based organometallic anticancer drugs, which can quench the PL of QDs when bound to the surface, were employed to detect various DNAs in a “turn off-on” manner (Fig. 9). Other quenching-type molecules, such as Nile blue<sup>62</sup> and cationic porphyrin,<sup>63</sup> also showed promise in detecting DNA with a “turn-on” PL. A copper free click chemistry was conducted to couple a single-stranded DNA to the surface of QD.<sup>64</sup> Then, FRET could be induced while a fluorophore-labelled complementary DNA probe was added, forming a double-stranded DNA on the surface of QDs. This hybridized sensor was used for both DNA and protein detections. Similarly, nucleic acid stabilized silver-nanocluster QDs were demonstrated for the multiplexed analysis of two DNAs.<sup>65</sup>

QDs were also used for determination of enzymatic activities. A fluorophore-labelled peptide was used as a substrate of

kallikrein, a key proteolytic enzyme for the blood clotting cascade, to self-assemble on QDs with a zwitterionic surface.<sup>66</sup> The FRET between the fluorophore label and QDs could be inhibited through digestion of the surface-coated peptide by the enzyme. On the basis of the same rationale, detection of the activity of human topoisomerase I was accomplished by a DNA coated QD.<sup>67</sup> A peptide coated gold cluster QD was used for detection of a protein kinase.<sup>68</sup> The presence of casein kinase II phosphorylated the serine residue of the surface-confined peptides, and a subsequent coordination with Zr<sup>4+</sup> using the phosphates led to PL quenching of the QDs.

Prostate specific antigen (PSA) is a biomarker for prostate cancer. An anti-PSA antibody coated QD, pre-conjugated with a quencher-labelled epitope peptide, was developed for the displacement-based detection of PSA.<sup>69</sup> A thrombin-aptamer coated QD, which showed a quenched PL with carbon nanodots due to FRET, was prepared.<sup>70</sup> It was shown that selective aptamer-thrombin interaction led to recovered PL, making possible a “turn-on” detection of the protein in biological fluids (Fig. 10). Ionic liquid functionalized silica-capped CdTe QDs were used for detection of hemoproteins by a PL quenching signal produced by the covalent interaction of the ionic liquid with the heme group.<sup>71</sup> A homogenous and fast detection protocol was established based on conjugation of conjoined protein binding agent/organic dye ligands to QDs for the quantitative detection of protein analytes.<sup>72</sup>

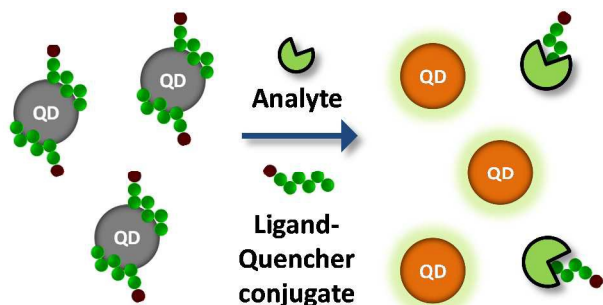


Figure 10. Detection of protein using the QD PL “turn off-on” rationale.

Sugar-lectin recognitions are important biological interactions that can manipulate a myriad of cellular events. Quinonyl glycosides with a thiol anchor were synthesized to coat QDs, quenching the PL by an ET mechanism.<sup>73</sup> Subsequent addition of a sugar receptor recovered the PL probably because of the encapsulation of the sugar-quinone quencher dyad by the protein, blocking the ET. The glycoquinone functionalized QDs were used for the selective imaging of live cancer cells that express a sugar receptor in a photoluminescent manner. Simultaneous detection of two sugar recognition proteins (lectins) was accomplished using a pair of QDs with different emission wavelength coated with different sugar ligands.<sup>74</sup> Based on a polymeric lectin-mediated QD aggregation, the dual QD emission could be quenched concomitantly upon the addition of both lectins.

QDs confined in a thin polymer film were constructed for PL-quenching based detection of glucose with a contact-free scheme.<sup>75</sup> The technique relied on formation of the fluores-

cent NADH, a byproduct of a hexokinase-6-phosphate dehydrogenase enzymatic glucose assay, to reduce the PL of QDs. The sensor was shown to operate over the entire clinical concentration range of glucose of human urine and whole blood. Boronate coated CdSe QDs, when bound with glycerol coated AuNPs, showed much more enhanced PL due to the surface plasmon resonance of the latter.<sup>76</sup> The presence of glucose competitively conjugated with the boronic QDs, leading to a weakened PL. While heparin (a negatively charged sulphated polysaccharide) has been used clinically for surgeries, its overdose might cause fatal complications. A ruthenium complex quencher was coated with QDs for the “turn-on” detection of heparin because of the strong electrostatic and hydrogen bonding interactions occurring between the complex and saccharide.<sup>77</sup> The properties of the QD based biomolecule sensors reviewed in this section are listed in Table 3.

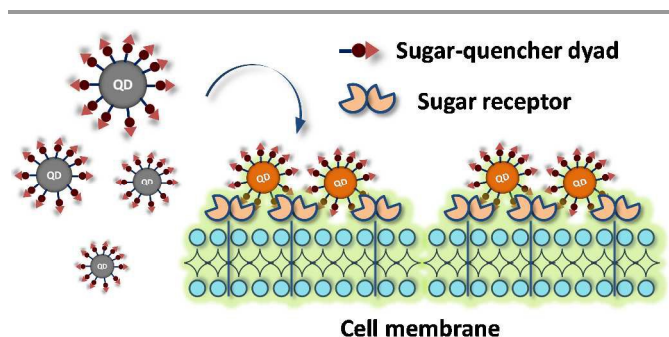


Figure 11. Detection of cell-membrane sugar receptors using QDs coated with a sugar-quencher dyad.

Table 3. Properties of the QD based sensors for biomolecules.

Analyte	Structure	CA <sup>a,b</sup>	LOD (μM) <sup>c</sup>	Ref <sup>f</sup>
DNA	CdTe	NAC	0.0011	60
	CdTe	NAC	n.a.	61
	CdTe	GSH	0.0028 <sup>d</sup>	62
Peptide	CdTe	TGA	0.0027	63
	CdSe/ZnS	DHLA	0.00009	64
	Ag cluster	NA	0.001	65
	CdSe/ZnS	DHLA	n.a.	66
	Qdot 605 ITK <sup>TM</sup>	n.a.	0.00025 <sup>d</sup>	67
Enzyme	Au cluster	Peptide	0.027 <sup>e</sup>	68
	Qdot	n.a.	n.a.	69
Protein	Mn-doped ZnS	MPA	0.000013	70
	CdTe	Silica	n.a.	71
	CdSe/ZnS	Silane	0.00004	72
Sugar	CdSe/ZnS	Glycoquinone	n.a.	73
	n.a.	n.a.	0.0003	74
	n.a.	n.a.	3.5	75
	CdSe	MPA	1860	76
	CdTe	TGA	0.00068	77

<sup>a</sup>CA means capping agent; <sup>b</sup>Abbreviation: NAC = *N*-acetyl-L-cysteine; GSH = glutathione; TGA = thioglycolic acid; NA = nucleic acid; DHLA = dihydroplipic acid; MPA = 3-mercaptopropionic acid; <sup>c</sup>LOD means limit of detection; <sup>d</sup>μg mL<sup>-1</sup>; <sup>e</sup>unit mL<sup>-1</sup>; <sup>f</sup>Reference (Ref) number cited in the main text.

### 3.2. QD based biosensors for live cell imaging

By taking advantage of the superior optical properties including high signal brightness and photostability, bio-functionalized

QDs have been used for cellular imaging. QDs decorated with a targeting agent that can facilitate the uptake of the QD by specific cells and/or with a reactive site with the ability to interact with a defined intracellular species have been extensively prepared for the "target-specific" imaging of live cells.

A chitosan-*O*-phospho-L-serine coated QD was prepared for imaging human bone marrow stromal cells.<sup>78</sup> The QDs with no cytotoxicity for the cells could be further used for PL detection of tissue regeneration and metabolic events. Since water soluble QDs are needed for biological applications, hydrophilic ZnCuInS/ZnS QDs<sup>79</sup> and CdTe QDs capped with a mixture of organic acids<sup>80</sup> were prepared for both *in vitro* cellular staining and *in vivo* imaging of tumors. Meanwhile, gadolinium labelled silica coated QDs were prepared for a concerted magnetic resonance and PL imaging of cancer cells.<sup>81</sup>

Studies that focus on target-specific imaging of cellular species have also been reported. In addition to targeting transmembrane receptors of cancer cells using glycoquinone coated QDs,<sup>73</sup> biofunctionalized QDs were prepared for probing intracellular enzymes. Mitochondrial NADH:ubiquinone oxidoreductase (complex I) is tightly implicated in the Parkinson's disease. Ubiquinone coated CdSe/ZnS QDs were constructed.<sup>82</sup> With NADH, complex I could modulate the electrochemistry of the surface-coated quinone/hydroquinone redox couple, leading to a PL change as an optical signal to image human neuroblastoma cells.

For protease detection in cells, streptavidin coated QDs and monomaleimide coated nanogold were linked via a caspase-3 selective substrate peptide to quench the PL of QDs by FRET.<sup>83</sup> Epidermal growth factor (EGF) was used to target the EGF receptors on cancer cells, enhancing the endocytosis efficiency. Finally the endocytosed nanoparticle complexes could be cleaved by caspase-3 to restore the PL. For *in vivo* application, aptamer labelled<sup>84</sup> and anti-A $\beta$  antibody coated<sup>85</sup> QDs were prepared for imaging a xenograft and senile plaques formed in mouse models, respectively. Targeted *in vivo* imaging of glioblastoma and prostate cancer angiogenesis using vascular endothelial growth factor antibody bioconjugated Ag<sub>2</sub>S QDs<sup>86</sup> and QDs coated with anti-vascular endothelial growth factor receptor 2 antibody<sup>87</sup> were also realized, respectively.

Multifunctional QDs with both imaging and suppression properties towards cancer cells were developed for disease theranostics. Cys-CdTe QDs loaded with gambogic acid, an anticancer drug, showed enhanced drug accumulation in leukemia cells.<sup>88</sup> A composite structure containing gold nanoflowers, SiO<sub>2</sub> and QDs was constructed. In addition to its imaging ability, the structure also showed thermotherapeutic effect for breast cancer cells upon an NIR irradiation.<sup>89</sup>

### 3.3. QD based biosensors for *in vivo* applications

Although arguments remain against the real application of QDs *in vivo* to complement current clinical contrast agents, attempts on evaluating the imaging ability of QDs with animal models have been extensive. The readers are also directed to some recent comprehensive reviews on this particular subject.<sup>90-92</sup> Besides the target-specific *in vivo* imaging studies highlighted in the last section,<sup>79,80,84-87</sup> many other innovative investigations have been carried out.

While the emission wavelength of the majority of currently used QDs falls into the first NIR window (650-950 nm) or below, QDs with a second NIR window emission (1000-1400 nm) have

been developed. Thanks to their deeper photon penetration, these materials are believed to offer greater promise for tissue and *in vivo* imaging.<sup>93</sup> Polyethylene glycol (PEG) coated Ag<sub>2</sub>S QDs with >1000 nm emission wavelength were prepared for evaluation of their toxicity *in vivo*.<sup>94</sup> It was shown that, over a period of 2 months, the QDs did not cause appreciable toxicity to mice, which suggested their potential for *in vivo* imaging. PbS/CdS QDs (ca. 1300 nm emission) with an improved quantum yield was fabricated, which showed high signal-to-background ratio and low blurring for *in vivo* imaging.<sup>95</sup> Ag<sub>2</sub>S QDs with the ability to visualize tissue blood flow and angiogenesis,<sup>96</sup> and a novel type of Ag<sub>2</sub>Se QDs with a 1000-1500 nm emission window were also developed.<sup>97</sup>

To address the toxicity issue of heavy-metal based QD materials, InP/ZnS QDs<sup>98</sup> and silicon QDs<sup>99</sup> were prepared and evaluated systematically for their *in vivo* toxicity towards mice and/or monkeys. Both were proven to be safer than traditional CdSe QDs. As an organic alternative of inorganic QDs, far-red/near infrared dots with aggregation-induced emission (AIE dots) were developed, showing promising properties such as high emission efficiency, strong photobleaching resistance as well as good biocompatibility.<sup>100</sup>

## 4. New trends

In addition to the conventional application of QDs as chemo- and biosensors, some new trends of using these materials are noteworthy. Of much interest is the synthesis of QDs by living organisms. It was shown that the earthworm's metal detoxification pathway was suited for producing CdTe QDs.<sup>101</sup> In addition to the QDs with a second NIR window emission, the combination of upconversion materials with QDs for biosensing represents another elegant strategy for developing biosensors. In particular, the combination yields NIR emissions, low background signal and thus a lowered detection limit.<sup>102</sup>

On the basis of their photophysical advantages, QDs have been employed in the development of diagnostic tools. In particular, QDs have been used as organic dye surrogates in immunoassays for detection of disease markers. By taking advantage of the Tb-to-QD FRET, antibody-coupled Tb and QD were used to form a sandwich complex with the prostate marker PSA with an LOD below the clinical cutoff line.<sup>103</sup> QD were also co-doped with other materials for immunoassays. Microbeads were extensively used to encapsulate QDs due to their advantages such as better quality control and solution kinetics and less sample requirement.<sup>104</sup> QD barcode assays using microfluidics and magnetism were established for point-of-care diagnosis of HIV, hepatitis B and syphilis.<sup>105</sup> Notably, a multicolor multicycle *in situ* imaging technology was developed, which enabled the molecular profiling of individual cells in a quantitative manner.<sup>106</sup>

Luminescent enhanced QD beads and liposomes loaded with QDs were prepared for the immunochromatographic detection of trace aflatoxin B<sub>1</sub> in maize<sup>107</sup> and determination of a food contaminant.<sup>108</sup> Notably, considering that most of the endoscopic diagnosis is based on the clinician's naked eye, antibody coated QDs were used to spray and wash colon tumor tissues inside live animals.<sup>109</sup> This provided an advantage for detecting small or flat tumors.

Finally, the employment of QDs in fingerprint detection has been highlighted in the forensic literature. ZnS:Cu QDs<sup>110</sup> and

hierarchical SiO<sub>2</sub>-QDs@SiO<sub>2</sub> nanostructures<sup>111</sup> were applied for visualization of (blood) fingerprints, offering a “brighter” means for forensics than conventional techniques.

## 5. Summary and perspective

In this review we have briefly summarized the development of QDs for application in a variety of practical fields over the past two years. These fields include the PL sensing of chemical pollutants and biologically important species, cellular and *in vivo* imaging, disease diagnosis and forensics. Despite the many elegant investigations, some essential problems remain, hampering the commercialization of QD sensors.

First, for analyte detection, the majority of the developed QD sensors are PL-quenching based. This “off-mode” signal might not be accurate enough for real application since in the complex biological system, non-specific PL quenching may frequently occur. Although other QD sensors with an “on-mode” signal have been developed, most of the systems dissemble upon interaction with an analyte. This might also lead to production of false-positive signals in a bio-system. More decent “on-type” detection rationales that could overcome the above drawbacks are needed.

Second, sensor standardization represents another main obstacle posing against the commercialization of these nanomaterials. Although standard procedures for producing a QD itself have been relatively mature, those for their biofunctionalization might require further improvement. For example, in the covalent coupling of an antibody to the surface of QDs, one can hardly precise that each QD particle would coat a similar amount of antibodies with an identically well-defined distribution manner. These factors would cause irreproducibility of the QD sensors from batch to batch.

Last but not the least, toxicity, a long-standing issue against QDs’ biomedical applications should be carefully examined.<sup>112</sup> Efforts have been made by use of relatively less toxic elements to fabricate a QD, even for QDs with an emission over the second NIR window. Alternatively, the development of core-shell QD structures has been vivid. Indeed, in addition to preventing surface traps and to improving stability of QDs, the development of metal semiconductor core-shell structures can minimize the potential toxicity of the conventional core materials consisting of heavy metals in biomedical applications. These core-shell structures have been realized chemically,<sup>113</sup> electrochemically<sup>114,115</sup> and physically,<sup>116</sup> and applied in sensitive detection of gases.<sup>117-119</sup>

However, discrepancy exists between cell culture and animal studies.<sup>112</sup> As proposed in a recent account, rather than simply asking “are QDs toxic?”,<sup>112</sup> standardized and systematized methodologies to assess the safety of each specific QD material (which is a combination of a core-shell structure, a capping agent, a receptor, a targeting agent, etc.), must be carefully established.

The authors are looking forward to elegant design strategies and applications of QD nanosensors or incorporated devices for clinical diagnosis as well as for detection of sugar-lectin recognitions,<sup>120-128</sup> a class of pivotal biological events that control cell fate. Use of sugars as a targeting agent for target-specific imaging of cellular species<sup>73,129,130</sup> could also be considered as a promising strategy for QD based sensor design.

## Acknowledgements

This research is supported by the 973 project (2013CB733700), the National Natural Science Foundation of China (21176076, 21202045), the Key Project of Shanghai Science and Technology Commission (13NM1400900) and the Fundamental Research Funds for the Central Universities.

## Notes and references

<sup>a</sup> College of Science, School of Environment and Architecture, University of Shanghai for Science and Technology, 516 Jungong Rd., Shanghai 200293, PR China

<sup>b</sup> Key Laboratory for Advanced Materials & Institute of Fine Chemicals, East China University of Science and Technology (ECUST), 130 Meilong Rd., Shanghai 200237, PR China

Email: [xphe@ecust.edu.cn](mailto:xphe@ecust.edu.cn) (X.-P. He), [mrs\\_guorongchen@ecust.edu.cn](mailto:mrs_guorongchen@ecust.edu.cn) (G.-R. Chen)

- 1 A. P. Alivisatos, *Science*, 1996, **271**, 933-937.
- 2 I. L. Medintz, H. T. Uyeda, E. R. Goldman and H. Mattoussi, *Nat. Mater.*, 2005, **4**, 435-446.
- 3 C. Suksai and T. Tuntulani, *Chem. Soc. Rev.*, 2003, **32**, 192-202.
- 4 L. Fabbrizzi, M. Licchelli, G. Rabaioli and A. Taglietti, *Coord. Chem. Rev.*, 2000, **205**, 85-108.
- 5 P. D. Beer, *Acc. Chem. Res.*, 1998, **31**, 71-80.
- 6 K. Huang, C. Jiang and A. A. Martí, *J. Phys. Chem. A*, 2014, **118**, 10353-10358.
- 7 J. Wang, *Electroanalysis*, 2005, **17**, 7-14.
- 8 C. B. Jacobs, M. J. Peairs and B. J. Venton, *Anal. Chim. Acta*, 2010, **662**, 105-127.
- 9 A. Saha, C. Jiang and A. A. Martí, *Carbon*, 2014, **79**, 1-18.
- 10 X.-P. He, Y. Zang, T. D. James, J. Li and G.-R. Chen, *Chem. Soc. Rev.*, DOI: 10.1039/c4cs00252k.
- 11 M. Pumera and A. H. Loo, *Trends Anal. Chem.*, 2014, **61**, 49-53.
- 12 I. Yildiz, M. Tomasulo and F. M. Raymo, *Proc. Natl. Acad. Sci. USA*, 2006, **103**, 11457-11460.
- 13 Y. Ding, S. Z. Shen, H. Sun, K. Sun and F. Liu, *Sens. Actuators, B*, 2014, **203**, 35-43.
- 14 A. S. Lima, S. S. M. Rodrigues, M. G.A. Korn, D. S.M. Ribeiro, J. L.M. Santos and L. S.G. Teixeira, *Microchem. J.*, 2014, **117**, 144-148.
- 15 D. Wu, Z. Chen, G. Huang and X. Liu, *Sens. Actuators, A*, 2014, **205**, 72-78.
- 16 H. Abdollahi, M. Shamsipur and A. Barati, *Spectrochim. Acta, Part A*, 2014, **127**, 137-143.
- 17 L.-H. Jin and C.-S. Han, *Anal. Chem.*, 2014, **86**, 7209-7213.
- 18 S. M. Ng, D. S. N. Wong, J. H. C. Phung and H. S. Chua, *Talanta*, 2013, **116**, 514-519.
- 19 J. Zhao, J. Ding, Y. Yi, H. Li, Y. Zhang and S. Yao, *Talanta*, 2014, **125**, 372-377.
- 20 H. Jiao, L. Zhang, Z. Liang, G. Peng and H. Lin, *Microchim. Acta*, 2014, **181**, 1393-1399.
- 21 C. Cai, H. Cheng, Y. Wang and H. Bao, *RSC Adv.*, 2014, **4**, 59157-59163.
- 22 M. S. Hosseini and A. Pirouz, *Luminescence*, 2014, **29**, 798-804.
- 23 Q. Mu, Yan, L., H. Xu, Y. Ma, W. Zhu and X. Zhong, *Talanta*, 2014, **119**, 564-571.

- 24 W. Bian, J. Ma, Q. Liu, Y. Wei, Y. Li, C. Dong and S. Shuang, *Luminescence*, 2014, **29**, 151-157.
- 25 L. Zi, Y. Huang, Z. Yan and S. Liao, *J. Lumin.*, 2014, **148**, 359-363.
- 26 R.-Y. Wang, J. Wu, L.-J. Wang, R. Wang and H.-J. Dou, *Spectrosc. Lett.*, 2014, **47**, 439-445.
- 27 J. Han, X. Bu, D. Zhou, H. Zhang and B. Yang, *RSC Adv.*, 2014, **4**, 32946-32952.
- 28 T. Zhao, X. Hou, Y.-N. Xie, L. Wu and P. Wu, *Analyst*, 2013, **138**, 6589-6594.
- 29 T.-W. Sung, Y.-L. Lo and I.-L. Chang, *Sens. Actuators, B*, 2014, **202**, 1349-1356.
- 30 Q. Ma, Z.-H. Lin, N. Yang, Y. Li and X.-G. Su, *Acta Biomater.*, 2014, **10**, 868-874.
- 31 Z. Liu, G. Li, Q. Ma, L. Liu and X. Su, *Microchim. Acta*, 2014, **181**, 1385-1391.
- 32 X. Luo, W. Wu, F. Deng, D. Chen, S. Luo and C. Au, *Microchim. Acta*, 2014, **181**, 1361-1367.
- 33 S. Xu, S. Xu, Y. Zhu, W. Xu, P. Zhou, C. Zhou, B. Dong and H. Song, *Nanoscale*, 2014, **6**, 12573-12579.
- 34 H. Qu, L. Gao, G. Su, W. Liu, R. Gao, C. Xia and J. Qin, *J. Nanopart. Res.*, 2014, **16**, 2762.
- 35 H.-L. Lee, N. Dhenadhyalan and K.-C. Lin, *RSC Adv.*, 2015, **5**, 4926-4933.
- 36 D. Zhao, X. Wan, H. Song, L. Hao, Y. Su and Y. Lv, *Sens. Actuators, B*, 2014, **197**, 50-57.
- 37 F. Shi, S. Liu and X. Su, *Talanta*, 2014, **125**, 221-226.
- 38 J. Yang, S. Liu, L. Wang, C. Hao, H. Gong, Y. Shen and Y. He, *Spectrosc. Lett.*, 2015, **48**, 351-358.
- 39 M.-R. Chao, C.-W. Hu and J.-L. Chen, *Microchim. Acta*, 2014, **181**, 1085-1091.
- 40 Y. Zhang, Y. Tang, X. Liu, Z. Zhang and Y. Lv, *Sens. Actuators, B*, 2013, **185**, 363-369.
- 41 R. Gui, H. Jin, X. Liu, Z. Wang, F. Zhang, J. Xia, M. Yang and S. Bi, *Chem. Commun.*, 2014, **50**, 14847-14850.
- 42 U. S. Akshath, L. R. Shubha, P. Bhatt and M. S. Thakur, *Biosens. Bioelectron.*, 2014, **57**, 317-323.
- 43 X. Wei, Z. Zhou, J. Dai, T. Hao, H. Li, Y. Xu, L. Gao, J. Pan, C. Li and Y. Yan, *J. Lumin.*, 2014, **155**, 298-304.
- 44 S. Han, X. Li, Y. Wang and S. Chen, *RSC Adv.*, 2015, **5**, 2129-2136.
- 45 X. Tan, S. Liu, Y. Shen, Y. He and J. Yang, *Spectrochim. Acta, Part A*, 2014, **133**, 66-72.
- 46 S. Liu, T. Gu, J. Fu, X. Li, I. S. Chronakis and M. Ge, *Mater. Sci. Eng. C*, 2014, **45**, 37-44.
- 47 O. L. Stroyuk, A. V. Yakovenko, O. E. Raevskaya and V. F. Plyusinin, *Phys. B*, 2014, **453**, 127-130.
- 48 S. Liu, F. Shi, X. Zhao, L. Chen and X. Su, *Biosens. Bioelectron.*, 2013, **47**, 379-384.
- 49 Q. Zhou, S.-Z. Kang, X. Li, L. Wang, L. Qin and J. Mu, *Colloids Surf., A*, 2015, **465**, 124-129.
- 50 S. Huang, F. Zhu, Q. Xiao, W. Su, J. Sheng, C. Huang and B. Hu, *RSC Adv.*, 2014, **4**, 46751-46761.
- 51 F. Long, H. Shi and H. Wang, *RSC Adv.*, 2014, **4**, 2935-2941.
- 52 A. H. Gore, M. B. Kale, P. V. Anbhule, S. R. Patil and G. B. Kolekar, *RSC Adv.*, 2014, **4**, 683-692.
- 53 M. Li, M. Ma, X. Hua, H. Shi, Q. Wang and M. Wang, *RSC Adv.*, 2015, **5**, 3039-3044.
- 54 X. Yan, H. Li, Y. Yan and X. Su, *Food Chem.*, 2015, **173**, 179-184.
- 55 J. Zhao, H. Wu, J. Jiang and S. Zhao, *RSC Adv.*, 2014, **4**, 61667-61672.
- 56 Y. Gong and Z. Fan, *Sens. Actuators, B*, 2014, **202**, 638-644.
- 57 B. T. Huy, M.-H. Seo, X. Zhang and Y.-I. Lee, *Biosens. Bioelectron.*, 2014, **57**, 310-316.
- 58 X. Ren and L. Chen, *Biosens. Bioelectron.*, 2015, **64**, 182-188.
- 59 S. Liu, S. Pang, H. Huang and X. Su, *Analyst*, **139**, 5852-5857.
- 60 S. Huang, F. Zhu, H. Qiu, Q. Xiao, Q. Zhou, W. Su and B. Hu, *Colloids Surf., B*, 2014, **117**, 240-247.
- 61 D. Zhao, J. Li, T. Yang and Z. He, *Biosens. Bioelectron.*, 2014, **52**, 29-35.
- 62 Y. Shen, S. Liu, L. Kong, X. Tan, Y. He and J. Yang, *Analyst*, 2014, **139**, 5858-5867.
- 63 E. Vaishnavi and R. Renganathan, *Analyst*, 2014, **139**, 225-234.
- 64 H. Zhang, G. Feng, Y. Guo and D. Zhou, *Nanoscale*, 2013, **5**, 10307-10315.
- 65 N. Enkin, F. Wang, E. Sharon, H. B. Albada and I. Willner, *ACS Nano*, 2014, **8**, 11666-11673.
- 66 J. C. Breger, K. E. Sapsford, J. Ganek, K. Susumu, M. H. Stewart and I. L. Medintz, *ACS Appl. Mater. Interfaces*, 2014, **6**, 11529-11535.
- 67 M. L. Jepsen, A. Ottaviani, B. R. Knudsen and Y.-P. Ho, *RSC Adv.*, 2014, **4**, 2491-2494.
- 68 W. Song, Y. Wang, R.-P. Liang, L. Zhang and J.-D. Qiu, *Biosens. Bioelectron.*, 2015, **64**, 234-240.
- 69 N. Frascione, J. Gooch, V. Abbate and B. Daniel, *RSC Adv.*, 2015, **5**, 6595-6598.
- 70 L. Zhang, P. Cui, B. Zhang and F. Gao, *Chem. Eur. J.*, 2013, **19**, 9242-9250.
- 71 D.-Y. Li, Y.-Z. Wang, X.-L. Zhao, X.-W. He, W.-Y. Li and Y.-K. Zhang, *J. Mater. Chem. B*, 2014, **2**, 5659-5665.
- 72 C. M. Tyrakowski and P. T. Snee, *Anal. Chem.*, 2014, **86**, 2380-2386.
- 73 W. Ma, H.-T. Liu, X.-P. He, Y. Zang, J. Li, G.-R. Chen, H. Tian and Y.-T. Long, *Anal. Chem.*, 2014, **86**, 5502-5507.
- 74 H. Zhang, L. Zhang, R.-P. Liang, J. Huang and J.-D. Qiu, *Anal. Chem.*, 2013, **85**, 10969-10976.
- 75 S. A. Khan, G. T. Smith, F. Seo and A. K. Ellerbee, *Biosens. Bioelectron.*, 2015, **64**, 30-35.
- 76 Y. Tang, Q. Yang, T. Wu, L. Liu, Y. Ding and B. Yu, *Langmuir*, 2014, **30**, 6324-6330.
- 77 Y. Cao, S. Shi, L. Wang, J. Yao and T. Yao, *Biosens. Bioelectron.*, 2014, **55**, 174-179.
- 78 C. L. Salgado, A. A. P. Mansur, H. S. Mansur and F. J. M. Monteiro, *RSC Adv.*, 2014, **4**, 49016-49027.
- 79 W. Guo, N. Chen, C. Dong, Y. Tu, J. Chang and B. Zhang, *RSC Adv.*, 2013, **3**, 9470-9475.
- 80 Y. Wang, R. Hu, G. Lin, W.-C. Law and K.-T. Yong, *RSC Adv.*, 2013, **3**, 8899-8908.
- 81 B. Lin, X. Yao, Y. Zhu, J. Shen, X. Yang and C. Li, *RSC Adv.*, 2014, **4**, 20641-20648.
- 82 W. Ma, L.-X. Qin, F.-T. Liu, Z. Gu, J. Wang, Z. G. Pan, T. D. James and Y.-T. Long, *Sci. Rep.*, 2013, **3**, 1537.
- 83 D. Ren, J. Wang and Z. You, *RSC Adv.*, 2014, **4**, 54907-54918.
- 84 C. Zhang, X. Ji, Y. Zhang, G. Zhou, X. Ke, H. Wang, P. Tinnefeld and Z. He, *Anal. Chem.*, 2013, **85**, 5843-5849.
- 85 L. Feng, H.-Y. Long, R.-K. Liu, D.-N. Sun, C. Liu, L.-L. Long, Y. Li, S. Chen and B. Xiao, *Cell. Mol. Neurobiol.*, 2013, **33**, 759-765.

- 86 Y. Wang and X. Yan, *Chem. Commun.*, 2013, **49**, 3324-3326.
- 87 H. Kwon, J. Lee, R. Song, S. I. Hwang, J. Lee, Y.-H. Kim and H. J. Lee, *Korean J. Radiol.*, 2013, **14**, 30-37.
- 88 J. Li, C. Wu, P. Xu, L. Shi, B. Chen, M. Selke, H. Jiang and X. Wang, *RSC Adv.*, 2013, **3**, 6518-6525.
- 89 T. Jiang, N. Yin, L. Liu, J. Song, Q. Huang, L. Zhu and X. Xu, *RSC Adv.*, 2014, **4**, 23630-23636.
- 90 C. E. Probst, P. Zrazhevskiy, V. Bagalkot and X. Gao, *Adv. Drug Delivery Rev.*, 2013, **65**, 703-718.
- 91 K.-T. Yong, W.-C. Law, R. Hu, L. Ye, L. Liu, M. T. Swihart and P. N. Prasad, *Chem. Soc. Rev.*, 2013, **42**, 1236-1250.
- 92 Y. Zhu, H. Hong, Z. P. Xu, Z. Li and W. Cai, *Curr. Mol. Med.*, 2013, **13**, 1549-1567.
- 93 E. Cassette, M. Helle, L. Bezdetnaya, F. Marchal, B. Dubertret and T. Pons, *Adv. Drug Delivery Rev.*, 2013, **65**, 719-731.
- 94 Y. Zhang, Y. Zhang, G. Hong, W. He, K. Zhou, K. Yang, F. Li, G. Chen, Z. Liu, H. Dai and Q. Wang, *Biomaterials*, 2013, **34**, 3639-3646.
- 95 Y. Tsukasaki, M. Morimatsu, G. Nishimura, T. Sakata, H. Yasuda, A. Komatsuzaki, T. M. Watanabe and T. Jin, *RSC Adv.*, 2014, **4**, 41164-41171.
- 96 C. Li, Y. Zhang, M. Wang, Y. Zhang, G. Chen, L. Li, D. Wu and Q. Wang, *Biomaterials*, 2014, **35**, 393-400.
- 97 B. Dong, C. Li, G. Chen, Y. Zhang, Y. Zhang, M. Deng and Q. Wang, *Chem. Mater.*, 2013, **25**, 2503-2509.
- 98 V. Brunetti, H. Chibli, R. Fiammengio, A. Galeone, M. A. Malvindi, G. Vecchio, R. Cingolani, J. L. Nadeau and P. P. Pompa, *Nanoscale*, 2013, **5**, 307-317.
- 99 J. Liu, F. Erogbogbo, K.-T. Yong, L. Ye, J. Liu, R. Hu, H. Chen, Y. Hu, Y. Yang, J. Yang, I. Roy, N. A. Karker, M. T. Swihart and P. N. Prasad, *ACS Nano*, 2013, **7**, 7303-7310.
- 100 K. Li, W. Qin, D. Ding, N. Tomczak, J. Geng, R. Liu, J. Liu, X. Zhang, H. Liu, B. Liu and B. Z. Tang, *Sci. Rep.*, 2013, **3**, 1150.
- 101 S. R. Stürzenbaum, M. Höckner, A. Panneerselvam, J. Levitt, J.-S. Bouillard, S. Taniguchi, L.-A. Dailey, R. Ahmad Khanbeigi, E. V. Rosca, M. Thanou, K. Suhling, A. V. Zayats and M. Green, *Nature Nanotech.*, 2013, **8**, 57-60.
- 102 For a recent comprehensive review, see: G. Chen, H. Qiu, P. N. Prasad and X. Chen, *Chem. Rev.*, 2014, **114**, 5161-5214.
- 103 K. D. Wegner, Z. Jin, S. Lindén, T. L. Jennings and N. Hildebrandt, *ACS Nano*, 2013, **7**, 7411-7419.
- 104 X. Wang, G. Wang, W. Li, B. Zhao, B. Xing, Y. Leng, H. Dou, K. Sun, L. Shen, X. Yuan, J. Li, K. Sun, J. Han, H. Xiao, Y. Li, P. Huang and X. Chen, *Small*, 2013, **9**, 3327-3335.
- 105 Y. Gao, A. W. Y. Lam and W. C. W. Chan, *ACS Appl. Mater. Interfaces*, 2013, **5**, 2853-2860.
- 106 P. Zrazhevskiy and X. Gao, *Nat. Commun.*, 2013, **4**, 1619.
- 107 M. Ren, H. Xu, X. Huang, M. Kuang, Y. Xiong, H. Xu, Y. Xu, H. Chen and A. Wang, *ACS Appl. Mater. Interfaces*, 2014, **6**, 14215-14222.
- 108 N. V. Beloglazova, P. S. Shmelin, E. S. Speranskaya, B. Lucas, C. Helmbrecht, D. Knopp, R. Niessner, S. D. Saeger and I. Yu. Goryacheva, *Anal. Chem.*, 2013, **85**, 7197-7204.
- 109 Y. Park, Y.-M. Ryu, Y. Jung, T. Wang, Y. Baek, Y. Yoon, S. M. Bae, J. Park, S. Hwang, J. Kim, E.-J. Do, S.-Y. Kim, E. Chung, K. H. Kim, S. Kim and S.-J. Myung, *ACS Nano*, 2014, **8**, 8896-8910.
- 110 S. Moret, A. Bécue and C. Champod, *Forensic Sci. Int.*, 2013, **224**, 101-110.
- 111 W. Dong, Y. Cheng, L. Luo, X. Li, L. Wang, C. Li and L. Wang, *RSC Adv.*, 2014, **4**, 45939-45945.
- 112 K. M. Tsoi, Q. Dai, B. A. Alman and W. C. W. Chan, *Acc. Chem. Res.*, 2013, **46**, 662-671.
- 113 Y. Lu, Y. Yin, Z.-Y. Li and Y. Xia, *Nano Lett.*, 2002, **2**, 785-788.
- 114 C. Gu, H. Xu, M. Park and C. Shannon, *Langmuir*, 2009, **25**, 410-414.
- 115 C. Gu, H. Xu, M. Park and C. Shannon, *ECS Trans.*, 2008, **16**, 181-190.
- 116 X. Y. Kong, Y. Ding and Z. L. Wang, *J. Phys. Chem. B*, 2004, **108**, 570-574.
- 117 H. Wang, Z. Sun, Q. Lu, F. Zeng and D. Su, *Small*, 2012, **8**, 1167-1172.
- 118 P. Fan, U. K. Chettiar, L. Cao, F. Afshinmanesh, N. Engheta and M. L. Brongersma, *Nat. Photonics*, 2012, **6**, 380-385.
- 119 Y.-S. Kim, P. Rai and Y.-T. Yu, *Sens. Actuators, B*, 2013, **186**, 633-639.
- 120 X.-P. He, X.-W. Wang, X.-P. Jin, H. Zhou, X.-X. Shi, G.-R. Chen and Y.-T. Long, *J. Am. Chem. Soc.*, 2011, **133**, 3649-3657.
- 121 H.-L. Zhang, X.-L. Wei, Y. Zang, J.-Y. Cao, S. Liu, X.-P. He, Q. Chen, Y.-T. Long, J. Li, G.-R. Chen and K. Chen, *Adv. Mater.*, 2013, **25**, 4097-4101.
- 122 Z. Li, S.-S. Deng, Y. Zang, Z. Gu, X.-P. He, G.-R. Chen, K. Chen, T.-D. James, J. Li and Y.-T. Long, *Sci. Rep.*, **3**, 2293.
- 123 B.-W. Zhu, L. Cai, X.-P. He, G.-R. Chen and Y.-T. Long, *Chem. Cent. J.*, 2014, **8**, 67.
- 124 X.-P. He, R.-H. Li, S. Maisonneuve, Y. Ruan, G.-R. Chen and J. Xie, *Chem. Commun.*, 2014, **50**, 14141-14144.
- 125 H.-L. Zhang, Y. Zang, J. Xie, J. Li, G.-R. Chen, X.-P. He and H. Tian, *Sci. Rep.*, **4**, 5513.
- 126 X.-L. Hu, H.-Y. Jin, X.-P. He, T. D. James, G.-R. Chen and Y.-T. Long, *ACS Appl. Mater. Interfaces*, 2015, **7**, 1874-1878.
- 127 Y. Hang, X.-P. He, L. Yang and J. Hua, *Biosens. Bioelectron.*, 2015, **65**, 420-426.
- 128 X.-P. He, B.-W. Zhu, Y. Zang, J. Li, G.-R. Chen, H. Tian and Y.-T. Long, *Chem. Sci.*, **6**, 1996-2001.
- 129 K.-B. Li, Y. Zang, H. Wang, J. Li, G.-R. Chen, T. D. James, X.-P. He and H. Tian, *Chem. Commun.*, 2014, **50**, 11735-11737.
- 130 D.-T. Shi, D. Zhou, Y. Zang, J. Li, G.-R. Chen, T. D. James, X.-P. He and H. Tian, *Chem. Commun.*, 2015, **51**, 3653-3655.